MR Imaging of the Penis and Scrotum[1]

Rex A. Parker III, MD
Christine O. Menias, MD
Robin Quazi, MD
Amy K. Hara, MD
Sadhna Verma, MD
Akram Shaaban, MD
Cary L. Siegel, MD
Alireza Radmanesh, MD
Kumar Sandrasegaran, MD

Abbreviations: ADC = apparent diffusion coefficient, DW = diffusion-weighted, FOV = field of view, FSE = fast spin-echo, GRE = gradient echo, SAR = specific absorption rate, STIR = short inversion time inversion-recovery, 3D = three-dimensional

RadioGraphics 2015; 35:1033–1050

Published online 10.1148/rg.2015140161

Content Codes: ER GU MR

[1]From the Department of Radiology, Kaiser Los Angeles Medical Center, 1526 N Edgemont St, 5th Floor, Los Angeles, CA 90027 (R.A.P.); Department of Radiology, Mayo Clinic Arizona, Scottsdale, Ariz (C.O.M., A.K.H.); Department of Radiology, University of California–Los Angeles, Los Angeles, Calif (R.Q.); Department of Radiology, University of Cincinnati, Cincinnati, Ohio (S.V.); Department of Radiology, University of Utah, Salt Lake City, Utah (A.S.); Mallinckrodt Institute of Radiology, Washington University School of Medicine, St Louis, Mo (C.L.S., A.R.); and Department of Radiology, Indiana University Medical Center, Indianapolis, Ind (K.S.). Presented as an education exhibit at the 2013 RSNA Annual Meeting. Received April 9, 2014; revision requested July 25 and received August 20; accepted September 23. For this journal-based SA-CME activity, the authors, editor, and reviewers have disclosed no relevant relationships. **Address correspondence to** R.A.P. (e-mail: *Rex.A.Parker@kp.org*).

SA-CME LEARNING OBJECTIVES

After completing this journal-based SA-CME activity, participants will be able to:

- Identify the basic anatomy of the penis and scrotum at MR imaging.
- Discuss clinical situations in which MR imaging may play a role in evaluating patients with known or suspected scrotal or penile disease.
- Describe MR imaging features that can aid in differentiating benign from malignant disease.

See www.rsna.org/education/search/RG.

Traditionally, due to its low cost, ready availability, and proved diagnostic accuracy, ultrasonography (US) has been the primary imaging modality for the evaluation of scrotal and, to a lesser extent, penile disease. However, US is limited by its relatively small useful field of view, operator dependence, and inability to provide much information on tissue characterization. Magnetic resonance (MR) imaging, with its excellent soft-tissue contrast and good spatial resolution, is increasingly being used as both a problem-solving tool in patients who have already undergone US and as a primary modality for the evaluation of suspected disease. Specifically, MR imaging can aid in differentiating between benign and malignant lesions seen at US, help define the extent of inflammatory processes or traumatic injuries, and play a vital role in locoregional staging of tumors. Consequently, it is becoming more important for radiologists to be familiar with the wide range of penile and scrotal disease entities and their MR imaging appearances. The authors review the basic anatomy of the penis and scrotum as seen at MR imaging and provide a basic protocol for penile and scrotal imaging, with emphasis on the advantages of MR imaging. Pathologic processes are organized into traumatic (including penile fracture and contusion), infectious or inflammatory (including Fournier gangrene and scrotal abscess), and neoplastic (including both benign and malignant scrotal and penile tumors) processes.

Introduction

Traditionally, owing to its low cost, ready availability, and proved diagnostic accuracy, ultrasonography (US) has been the primary modality for imaging of the penis and scrotum (1,2). However, US is limited by its relatively small useful field of view (FOV), operator dependence, and inability to provide much information on tissue characterization. Consequently, as magnetic resonance (MR) imaging has become more readily available and more widely accepted by urologists, it is increasingly being used as a problem-solving adjunct. The large FOV and multiplanar capability of MR imaging

TEACHING POINTS

- The tunica albuginea remains intact in penile contusion, and close attention to this structure is warranted to exclude fracture.
- When a scrotal hematoma or hematocele is present, the radiologist should be vigilant in looking for associated penile or testicular injury.
- With its excellent soft-tissue contrast, multiplanar capability, and relatively large FOV, MR imaging is a key tool in the localization of undescended testicles.
- The ability of MR imaging to help characterize soft tissue can help differentiate benign from malignant neoplasms or predict the presence of malignant disease.
- MR imaging is useful for defining the extent of penile cancer and assessing for invasion of the corpora cavernosa and/or urethra. Close attention should be paid to inguinal and pelvic lymph nodes, given the important prognostic implications of nodal involvement.

have long lent themselves to aiding in the preoperative localization of incompletely descended testes that are not palpable at physical examination (3). Moreover, US has proved inconclusive in up to 5% of cases of suspected scrotal disease (4), with MR imaging providing additional value in many of these instances. Some studies have even suggested that the performance of MR imaging following inconclusive US is cost effective (5). Specifically, MR imaging can help differentiate between benign and malignant lesions seen at US. The larger FOV of MR imaging can also allow delineation of tumor extent in cases of large masses and better visualization of locoregional metastatic disease. In addition, MR imaging has proved superior to physical examination in the staging of penile cancer (6). The ability of MR imaging to help characterize blood products of varying ages and depict the T1- and T2-hypointense tunica albuginea is a powerful advantage in cases of penile or scrotal trauma. Furthermore, defining the extent of inflammatory or infectious diseases and potentially identifying unexpected sources of infection represent advantages of MR imaging over US in patients with suspected abscess or Fournier gangrene.

In this article, we describe the basic anatomy of the penis and scrotum as seen at MR imaging; a basic protocol for penile and scrotal MR imaging; and the MR imaging appearances of benign and malignant processes of the penis and scrotum. We have organized the relevant pathologic processes into three general categories: *(a)* traumatic, including penile fracture and contusion; *(b)* infectious or inflammatory, including Fournier gangrene and scrotal abscess; and *(c)* neoplastic, including both benign and malignant penile and scrotal tumors.

Normal Anatomy

Penis

The penis consists of paired corpora cavernosa dorsally and a midline corpus spongiosum ventrally (Fig 1) (7). Proximally, the corpora cavernosa form crura that attach to the ischial tuberosities. The corpora cavernosa are composed of venous sinusoids whose purpose is to fill with blood during erection. The corpus spongiosum surrounds the penile urethra and forms the glans penis distally. At MR imaging, both the corpus spongiosum and the corpora cavernosa appear hyperintense on T2-weighted images and have intermediate signal intensity on T1-weighted images. The musculature of the urethra appears hypointense relative to the surrounding corpus spongiosum. Both the corpus spongiosum and the corpora cavernosa are enveloped by a strong fascial sheath known as the tunica albuginea. The tunica albuginea appears hypointense on both T1- and T2-weighted images. Following the intravenous administration of gadolinium-based contrast agents, both the corpus spongiosum and corpora cavernosa enhance. The cavernosal bodies demonstrate gradual enhancement with a centrifugal pattern, whereas the corpus spongiosum enhances early (8).

Scrotum

The scrotal sac is composed of multiple layers, including the skin, multiple muscle and fascial layers, and the tunica vaginalis (9,10). The tunica vaginalis is a two-layered serous membrane that derives from the processus vaginalis of the peritoneum: The visceral layer envelops the testicles and epididymis, whereas the parietal layer forms the inner lining of the scrotal sac. Fluid collections, such as hydroceles, form in the potential space between the layers of the tunica vaginalis. At MR imaging, the scrotal sac is typically hypointense on both T1- and T2-weighted images (Fig 2).

The normal adult testis is a homogeneous oval structure that appears hyperintense on T2-weighted MR images (Fig 2) and hypo- to isointense on T1-weighted images. The testis is surrounded by the T1- and T2-hypointense tunica albuginea. Relative to the testis, the epididymis is isointense on T1-weighted images but hypointense on T2-weighted images. Following the intravenous administration of gadolinium-based contrast agents, both the testicles and the epididymis enhance.

Imaging Technique

Appropriate patient positioning is essential for imaging of the penis and scrotum. Patients should be placed supine on the imaging table, with a towel placed between the upper thighs

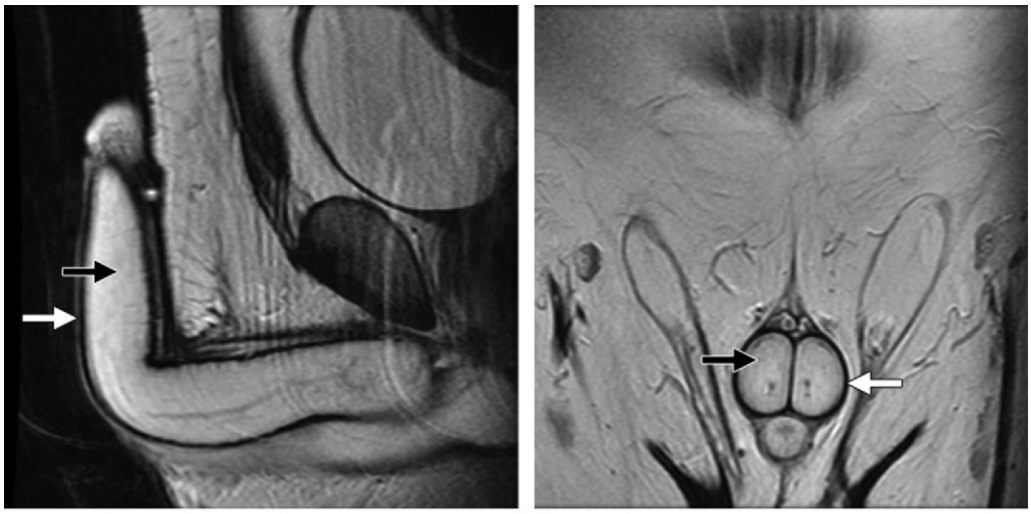

a. b.

Figure 1. Normal penile anatomy. Sagittal **(a)** and coronal **(b)** T2-weighted MR images show the corpora cavernosa and corpus spongiosum with high signal intensity (black arrow) and the surrounding tunica albuginea with low signal intensity (white arrow).

Figure 2. Normal scrotal anatomy. Coronal T2-weighted MR image shows homogeneously hyperintense testes (black arrow) beneath the more hypointense epididymis (arrowhead). The scrotal sac (white arrow) is hypointense, a normal finding on both T1- and T2-weighted images.

to elevate the scrotum. The penis is dorsiflexed against the anterior abdominal wall and is taped in place to prevent motion. A multiple phased-array surface coil is placed over the lower abdominopelvic wall and scrotum.

The Table outlines a basic protocol for MR imaging of the penis and scrotum, including additional imaging sequences that can be performed depending on clinical history. In general, we believe that protocols for imaging of the penis and/or scrotum should include a small (16-cm) FOV and thin-section (4-mm) non-fat-suppressed FSE T2-weighted sequences with relatively high resolution (matrix of 256 × 192 or higher) performed in the axial, coronal, and sagittal planes. The addition of full-FOV T2-weighted imaging through the pelvis is valuable in cases of known or suspected malignancy or infection. Some authors also advocate the addition of dual-echo (in- and opposed-phase) spoiled GRE T1-weighted imaging in the axial plane (11). The addition of this sequence may aid in identifying lesions that contain lipid, as well as provide improved characterization of blood products due to their T2* effects. In cases of a palpable abnormality or suspected mass, at least one fat-suppressed sequence should be included to aid in identifying macroscopic fat. Use of a fat-suppressed FSE or STIR T2-weighted sequence can also aid in identifying fluid collections or soft-tissue edema. In some cases (eg, for local staging of penile cancer), intravenous contrast material may not be necessary. For other indications, a 3D fat-suppressed spoiled GRE T1-weighted sequence is performed in the axial plane both before and after the intravenous administration of 0.1 mmol/kg of gadolinium-based contrast material. For staging of cancer or delineation of the extent of an infectious process, the addition of coronal and/or sagittal postcontrast 3D spoiled GRE imaging should be considered. The addition of axial DW imaging should also be considered in cases of suspected infection or tumor. Although the role of DW imaging has not been fully evaluated in the literature, this technique has shown promise in identifying an undescended testis and diagnosing suspected abscess. There is also growing

Protocol for Penile-Scrotal MR Imaging

Imaging Sequence and Planes	FOV (mm)	Section Thickness (mm)	Gap (mm)	Matrix Size	Applications
Standard anatomic sequences					
Axial, sagittal, coronal localizer	400	10	5	128 × 256	Prescription of subsequent sequences
Axial, coronal, sagittal T2W FSE	160	4	0.5	256 × 192	Core sequences for anatomic overview, localizing masses, evaluating the integrity of the tunica albuginea, characterizing masses and fluid collections
Axial T1W SE	340	5	1	256 × 192	Characterizing masses and fluid collections, evaluating the integrity of the tunica albuginea, assessing for deep pelvic disease as well as pelvic and inguinal adenopathy
Additional sequences for trauma					
Axial T1W dual-echo spoiled GRE (in phase and out of phase)	340	4	1	256 × 192	Better characterizing blood products due to T2* effects
Sagittal T2W fat-suppressed FSE or STIR	160	4	0.5	256 × 192	Identifying fluid collections and edema
Additional sequences for inflammation					
Axial DW	340	8	2	128 × 128	Characterizing fluid collections as abscesses
Axial T2W fat-suppressed FSE or STIR	340	6	1	320 × 256	Identifying fluid collections and edema
Axial postcontrast T1W 3D fat-suppressed spoiled GRE	340	3	0	320 × 256	Characterizing fluid collections, identifying sites of inflammation, delineating extent of inflammation, assessing for active inflammation in Peyronie disease
Additional sequences for tumor					
Axial T2W fat-suppressed FSE or STIR	160	4	0.5	256 × 192	Evaluating for macroscopic fat content in masses, identifying cystic masses and associated inflammation
Axial T1W dual-echo spoiled GRE (in phase and out of phase)	340	4	1	256 × 192	Better characterizing blood products due to T2* effects, evaluating for intracellular fat in tumors
Axial DW	340	8	2	128 × 128	Identifying tumor, assessing response to therapy
Axial pre- and postcontrast T1W fat-suppressed 3D spoiled GRE	340	3	0	320 × 256	Evaluating for enhancement of soft-tissue masses, assessing extent of tumor
Sagittal postcontrast T1W fat-suppressed 3D spoiled GRE	260	3	0	256 × 192	Evaluating for enhancement of soft-tissue masses, assessing extent of tumor

Note.—DW = diffusion-weighted, FSE = fast spin-echo, GRE = gradient-echo, SE = spin-echo, STIR = short inversion time inversion-recovery, 3D = three-dimensional, T1W = T1-weighted, T2W = T2-weighted.

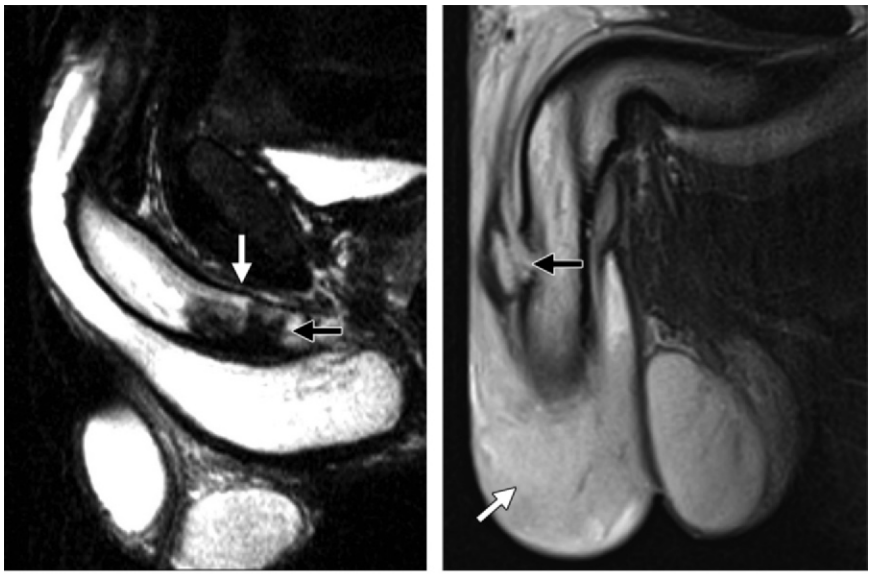

a. b.

Figure 3. Penile trauma. **(a)** Sagittal T2-weighted MR image in a 43-year-old man shows a focal region of low signal intensity in the left corpus cavernosum (black arrow) without disruption of the T1- and T2-hypointense tunica albuginea fibrous band (white arrow), findings that are consistent with penile contusion. **(b)** Sagittal T2-weighted MR image in a 17-year-old boy demonstrates focal disruption of the hypointense tunica albuginea of the left corpus cavernosum (black arrow) associated with a large hematocele (white arrow).

evidence in the literature to support the use of DW imaging in oncologic applications to help identify tumor and assess response to therapy.

Some authors advocate the intracavernosal injection of prostaglandin E1 to allow imaging of the erect penis (12,13). However, there are several contraindications to prostaglandin E1, including implants and conditions that predispose to priapism, such as sickle cell anemia. Although the associated risk of priapism is low (14), the use of prostaglandin E1 complicates workflow and requires more stringent patient screening. Consequently, we do not routinely image the erect penis.

Most modern penile implants, and all of the inflatable type, can be safely imaged with MR imaging. Two prostheses—OmniPhase and DuraPhase (Dacomed, Minneapolis, Minn)—have demonstrated deflection forces (15,16) and should not be imaged.

The biologic effects of MR imaging on the testis and on spermatogenesis are not clearly understood or well evaluated in the literature. Some studies performed on mice suggest that exposure to a static 1.5-T magnetic field can result in a temporary reduction in testicular sperm (17). In addition, although the radiofrequency radiation used in MR imaging is nonionizing, it can result in energy deposition and tissue heating. Energy deposited in the patient is referred to as the specific absorption rate (SAR) and is measured in watts per kilogram. The SAR is dependent on type of pulse sequence and magnetic field strength. A study dealing specifically with scrotal heating as a function of SAR demonstrated that imaging at relatively high SARs leads to increases in scrotal temperature of up to 3°C (18). However, it was noted that this temperature elevation did not reach the thresholds known to reduce sperm count in humans (18). It is important to recognize that the effects of MR imaging on the testis are not clear, and that there is potential for some deleterious effects. Consequently, as with other imaging modalities, it is prudent to weigh the risks and benefits of the study when considering whether to perform MR imaging of the scrotum.

Trauma

Penile fracture is defined as a tear in the tunica albuginea with resultant rupture of the corpus cavernosum (10,19). Fracture can result from both blunt and penetrating trauma, although imaging of penetrating trauma to the penis is rare, since these injuries are usually associated with multiple other sites of trauma and are more frequently identified at surgical exploration (10). Most penile fractures occur as a result of powerful lateral motions of the erect penis, frequently during sexual intercourse (19). MR imaging demonstrates focal disruption of the T1- and T2-hypointense tunica albuginea, usually with an adjacent T2-hyperintense hematoma (Fig 3b) (10,20,21). MR imaging may prove superior to US in identifying the site and extent of tunica albuginea involvement. Importantly, penile fracture

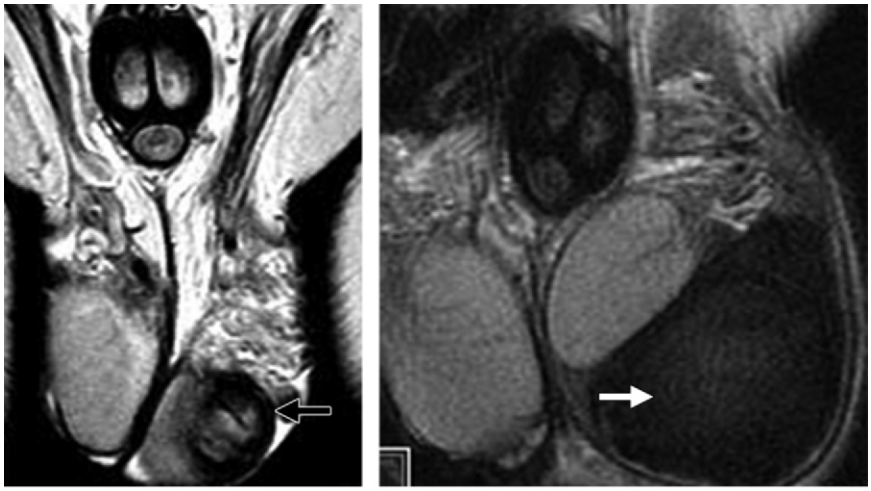

a. b.

Figure 4. Scrotal hematoma. **(a)** Coronal T2-weighted MR image in a 24-year-old man demonstrates a hematoma with a markedly hypointense hemosiderin rind in the left side of the scrotum (arrow). **(b)** Coronal T2-weighted MR image in a 22-year-old man shows a large, complex fluid collection with classic hypointense signal in the scrotum (arrow), a finding that is consistent with blood products.

is associated with urethral injury in 10%–20% of patients, an injury that is clinically suspected based on the presence of blood at the urethral meatus (22). If urethral injury is suspected, retrograde urethrography may be warranted, although some studies suggest that preoperative urethrography is unlikely to affect management and is probably unnecessary (23). Clinically, patients present with excruciating pain, bruising, and rapid detumescence. To avoid long-term complications such as painful erection, urethral stricture, or erectile dysfunction, urgent surgery is advocated (24).

MR imaging can sometimes be useful in differentiating penile fracture from the less serious penile contusion. At MR imaging, penile contusion manifests as a focal area of hypointensity in the normally T2-bright corpus cavernosum (Fig 3a). The tunica albuginea remains intact in penile contusion, and close attention to this structure is warranted to exclude fracture. There is typically less edema in the superficial soft tissues, and the presence of a large hematoma is unlikely. Differentiation between contusion and fracture is important, since fracture is treated surgically, whereas contusion is treated conservatively with nonsteroidal analgesics and application of ice packs (25).

Hematoceles occur when blood accumulates in the potential space between the visceral and parietal layers of the tunica vaginalis. Causes include both blunt and penetrating trauma, iatrogenic causes (typically related to surgery), and anticoagulation, as well as testicular fracture or potential testicular torsion. The imaging appearance of hematoceles at MR imaging varies depending on acuteness. In the early stages, one would expect hematoceles to be T2 hyperintense and, depending on the exact timing of imaging, T1 hyperintense (26). Over time, the blood products evolve and ultimately become T2 hypointense due to the presence of hemosiderin (Fig 4). If a dual-echo spoiled GRE T1-weighted sequence is included, one may see "blooming" that is more pronounced on the in-phase image due to progressive dephasing with the longer echo time. When a scrotal hematoma or hematocele is present, the radiologist should be vigilant in looking for associated penile or testicular injury.

Occasionally, a scrotal or spermatic cord hematoma may manifest as a mass (11). In such cases, MR imaging can be invaluable in accurately characterizing the mass based on the signal characteristics of blood products and the lack of enhancement following the intravenous administration of contrast material. Most scrotal hematomas resolve over time. Occasionally, surgical or percutaneous drainage may be warranted (27,28).

Testicular hematoma, fracture, and rupture typically occur in younger men and are often sports related (10). These injuries are typically suspected clinically based on patient history and results of physical examination. If imaging is necessary for confirmation or characterization, US is the first-line modality due to its ready availability and accuracy (29). Small studies have suggested that MR imaging has excellent sensitivity and specificity for diagnosing testicular rupture (30). However, given the proved accuracy of US and

Figure 5. Undescended testis. Sagittal T2-weighted MR image in a 44-year-old man demonstrates an undescended testis in the left inguinal canal (arrow).

the added time required for MR imaging, the use of MR imaging in cases of suspected testicular trauma is not recommended. Fracture or rupture of the testicle manifests as disruption of the normally T1- and T2-hypointense tunica albuginea, typically with adjacent hematoma.

Anatomic Abnormalities

Cryptorchidism is the absence of one or both testes in the scrotal sac. In roughly 4% of patients with cryptorchidism, the undescended testis (not palpable at physical examination) is either atrophic, absent, or perhaps intra-abdominal in location (31). With its excellent soft-tissue contrast, multiplanar capability, and relatively large FOV, MR imaging is a key tool in the localization of undescended testicles. The lack of ionizing radiation at MR imaging also represents a decided advantage over computed tomography (CT) in young patients. Accurate identification and localization is important for initiating appropriate therapy to maintain endocrine function as well as screen or treat associated neoplasms. A recent large meta-analysis confirmed this utility of MR imaging, which had a sensitivity of 62% for localizing an incompletely descended testis and an even higher sensitivity for testicles located in the inguinoscrotal region, with a specificity of 1 (3). At MR imaging, the undescended testicle has signal characteristics similar to those of testicles in the scrotum (ie, hyperintense on T2-weighted images [Fig 5] and hypo- to isointense on T1-weighted images). The spermatic cord or gubernaculum testis can be followed to aid in localization. Recent studies suggest that DW imaging may also aid in localization, since the undescended testicle is frequently markedly hyperintense on DW images obtained with high *b* values (b = 800 sec/mm^2) (32).

MR imaging can also play a role in the evaluation of other congenital abnormalities of the urogenital system (eg, ambiguous genitalia). However, description of these anomalies is beyond the scope of this article.

Infection

Epididymitis and epididymo-orchitis are common causes of acute scrotal pain, typically as a result of retrograde infection from a lower urinary tract infection (33). Given its excellent diagnostic accuracy and ready availability, US remains the mainstay for imaging patients with suspected scrotal infection. However, MR imaging may prove useful as an adjunct in patients with suspected complications. Inadequately treated infection can lead to epididymal or testicular abscess or even venous infarction. The infection can break through the tunica vaginalis and lead to pyocele formation. At MR imaging, epididymitis appears as an enlarged, edematous epididymis with associated brisk hyperenhancement following contrast material administration. Inflammation in the adjacent soft tissues is typical, manifesting as wispy areas of increased T2 signal on fat-suppressed images.

Although scrotal-epididymal abscesses are readily seen at US, MR imaging may prove useful in defining the extent of infection or inflammation, thereby aiding in planning potential surgical débridement or percutaneous drainage. Abscesses manifest as deep, centrally T2-hyperintense fluid collections with variable T1 signal and peripheral enhancement (Figs 6, 7). As with abscesses elsewhere in the body (eg, in the liver or brain) (34,35), the abscess cavity demonstrates central hyperintensity on DW images with corresponding low signal on ADC maps, findings that are indicative of restricted diffusion. In cases of known or suspected abscess, MR imaging can also add value in defining sinus tracts or fistulous tracts to the skin. The appearance of fistulas elsewhere in the pelvis—specifically, perianal fistulas—has been well described in the literature (36). Fistulas associated with scrotal abscesses have a similar appearance, manifesting as hypointense linear structures on T1-weighted images with corresponding hyperintensity on fat-suppressed T2-weighted images (Fig 7) (36).

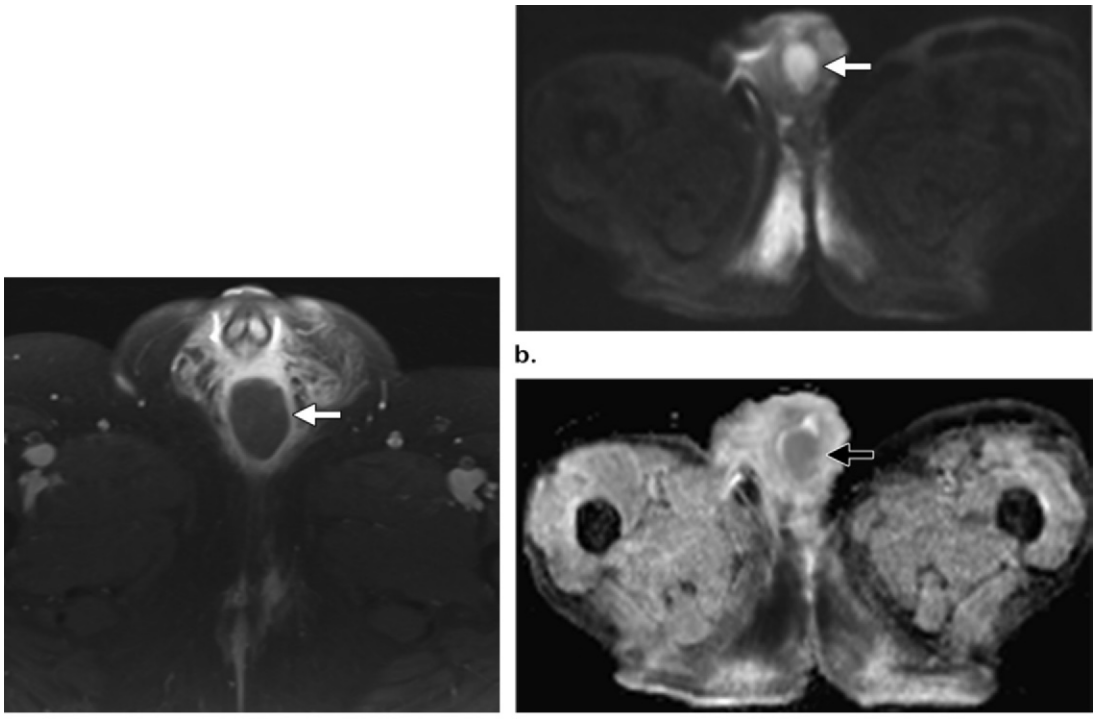

Figure 6. Scrotal abscess in a 40-year-old man. Axial postcontrast T1-weighted MR image **(a)**, DW image **(b)**, and apparent diffusion coefficient (ADC) map **(c)** show a deep, peripherally enhancing fluid collection at the base of the scrotum with associated diffusion restriction (arrow).

Penile and scrotal abscesses may also be iatrogenic, related to penile prosthesis placement, missed torsion, infected tumor, or extension from an abdominopelvic or subcutaneous source. Abscesses associated with these causes appear similar at imaging (Fig 8).

Fournier gangrene is a necrotizing perineal infection involving both superficial and deep fascial planes. It is associated with numerous comorbidities, notably diabetes mellitus (10,37). The high associated mortality rate, reported to be as high as 50% (38), makes Fournier gangrene a urologic emergency requiring rapid diagnosis. Potential sources of infection are numerous and include urinary tract infections, epididymitis, pressure ulcers, and gastrointestinal causes such as inflammatory bowel disease or perirectal abscess (10). Given its short acquisition time and its ability to help identify sources of infection and delineate disease extent, CT is the imaging modality of choice for Fournier gangrene (37). CT is also readily available in most emergency department settings and has the added advantage of helping clearly identify soft-tissue gas. MR imaging, because of its long acquisition time and provision of only limited information in addition to that provided by CT, should not be the primary imaging modality in patients with suspected Fournier gangrene. Nevertheless, MR imaging may occasionally be performed in cases in which clinical findings are unclear or another diagnosis is suspected. The appearance of Fournier gangrene at MR imaging is similar to that at CT, with extensive perineal inflammation, fascial thickening, soft-tissue gas, and, in some cases, fluid collections or fistulas (Fig 9). Inflammation appears as reticulation of the perineal fat with wispy increased T2 signal on fat-suppressed images. Soft-tissue gas can be identified at MR imaging as regions of signal void. Air-fluid levels may also be seen (Fig 9). The presence of gas results in susceptibility artifact due to local magnetic field heterogeneity, a finding that is more pronounced with GRE sequences and sequences involving longer echo times.

Inflammation

Peyronie disease is a chronic inflammatory condition that has been postulated to be the result of chronic penile trauma, likely related to shear forces on the tunica albuginea (39). Clinically, Peyronie disease typically has two phases: *(a)* an acute phase characterized by pain; and *(b)* a chronic phase characterized by penile deformity, typically with less pain (13,40). Plaques from Peyronie disease are typically palpable. At MR imaging, plaques appear as focal areas of T1- and T2-hypointense thickening of the tunica albuginea (Fig 10) (13). MR imaging and US are similar in terms of their ability to help detect plaques (41); however, MR imaging likely adds

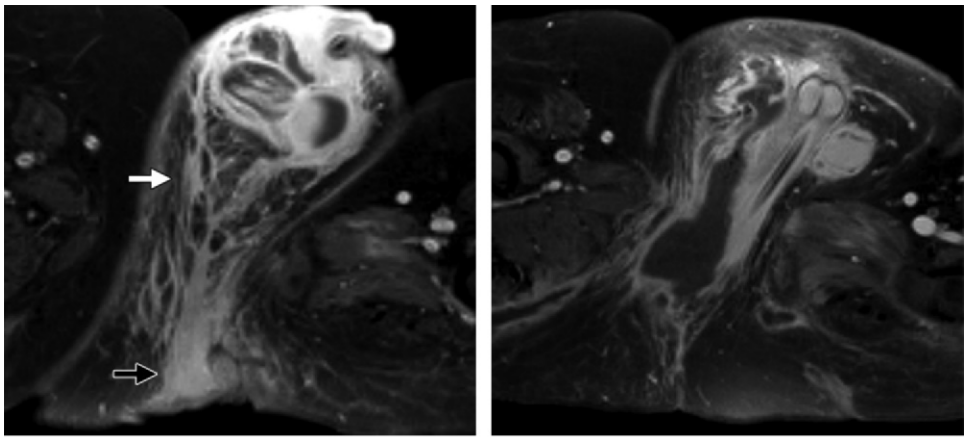

a. b.

Figure 7. Penile-scrotal abscess with cutaneous fistula in a 21-year-old man. **(a)** Axial postcontrast T1-weighted MR image shows extensive inflammation of the scrotum (white arrow) with a fistula to the skin surface (black arrow). **(b)** Axial postcontrast T1-weighted MR image shows a large, peripherally enhancing abscess at the base of the penis.

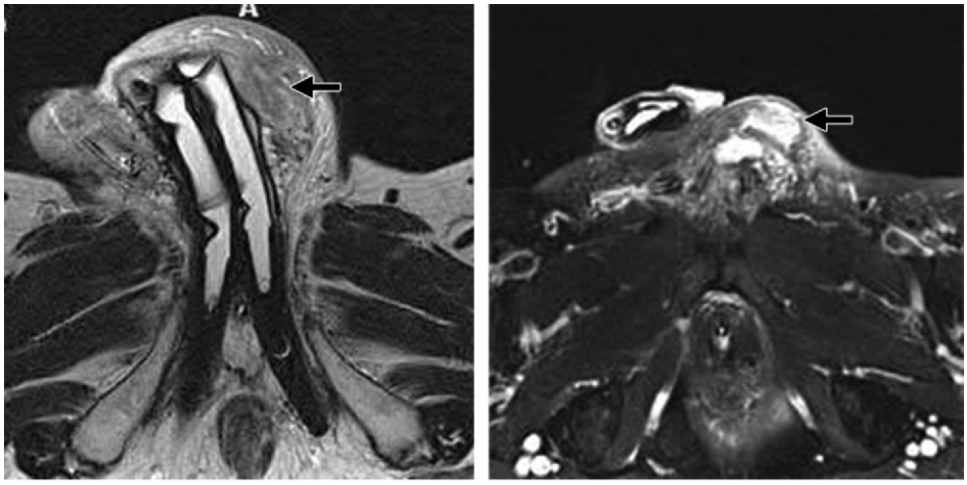

a. b.

Figure 8. Infected penile implant in a 67-year-old man. Axial T2-weighted **(a)** and axial fat-saturated T-weighted **(b)** MR images show peri-implant edema and fluid (arrow).

value by allowing more accurate assessment of plaque location and thickness, disease extent, and cavernosal diameter prior to surgery (13).

Some authors have also suggested that the enhancement of plaque following the intravenous administration of gadolinium-based agents can be used to identify patients with active inflammation (42). Although this hypothesis has not been fully evaluated in the literature, it suggests an intriguing possible advantage of MR imaging, since most surgeons prefer to postpone intervention until after the active inflammatory phase to minimize local recurrence (43).

Masses

MR imaging has numerous potential advantages over other imaging modalities—notably US—in the evaluation of suspected neoplastic processes of the penis and scrotum. First, the soft-tissue contrast of MR imaging provides excellent depiction of the penile and scrotal anatomy, allowing the radiologist to accurately assess the extent of tumor involvement. For instance, MR imaging has proved superior to physical examination in assessing the depth of cavernosal invasion in patients with penile cancer (6). Second, the ability of MR imaging to help characterize soft tissue can help differentiate benign from malignant neoplasms or predict the presence of malignant disease. In fact, some studies of the clinical utility of scrotal MR imaging suggest that the ability of this modality to help accurately identify malignant and benign neoplasms, inflammatory processes, and traumatic or fibrotic processes may be its most important role, especially given the sometimes confusing US appearance of the aforementioned benign entities (4).

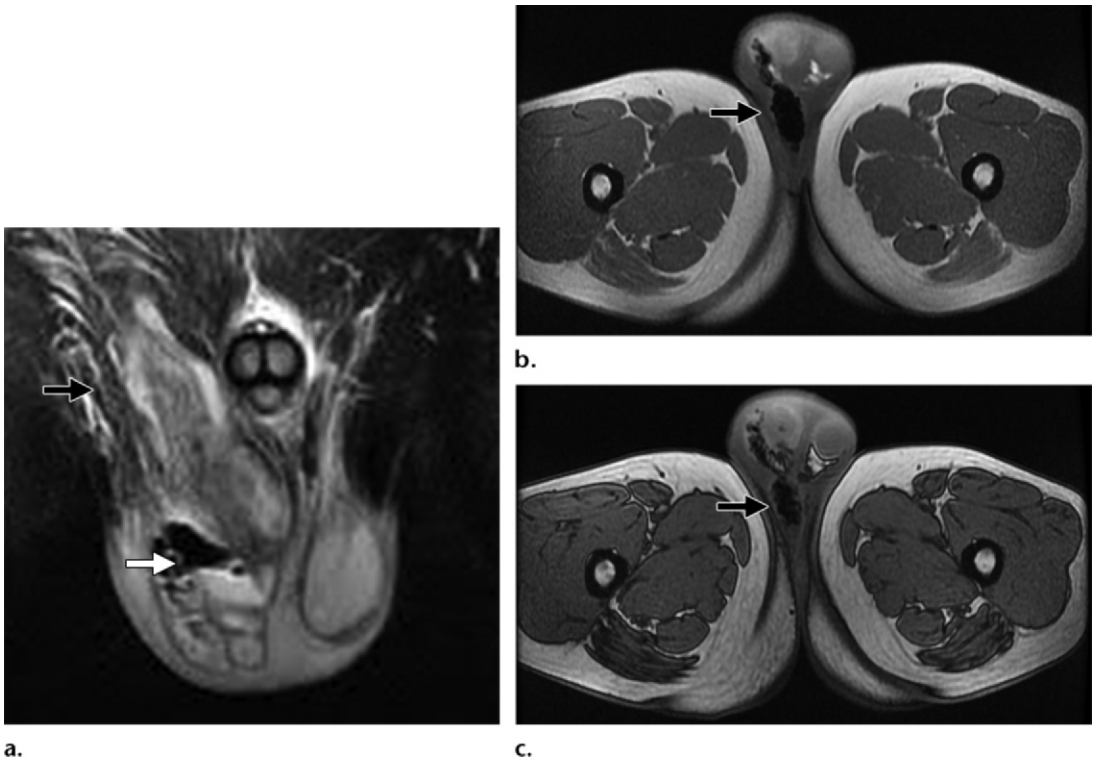

Figure 9. Fournier gangrene in a 47-year-old man. **(a)** Coronal fat-saturated T2-weighted MR image demonstrates diffuse edema of the perineum and scrotum (black arrow), with pockets of air and an air-fluid level seen in the right side of the scrotum (white arrow). **(b, c)** Axial in-phase **(b)** and opposed-phase **(c)** T1-weighted MR images demonstrate characteristic blooming (arrow) that is more pronounced in **b** due to progressive dephasing associated with the longer echo time used for in-phase imaging.

Figure 10. Peyronie disease in a 29-year-old man. Sagittal fat-saturated T2-weighted MR image demonstrates focal thickening and plaque of the tunica albuginea along the dorsum of the penis (arrow).

Scrotum

Lipomas are benign mesenchymal tumors that are predominantly composed of macroscopic fat. True lipomas are encapsulated fatty masses. At MR imaging, they appear homogeneously hyperintense on T1- and T2-weighted images and do not enhance following contrast material administration (11), with homogeneous loss of signal on fat-suppressed images (Fig 11). A few thin internal septa may be seen. The term *spermatic cord lipoma* refers to extrusions of extraperitoneal fat into the inguinal canal. Spermatic cord lipomas are not true tumors and are frequently confused with fat-containing inguinal hernias. MR imaging and CT can both help distinguish true paratesticular lipomas and spermatic cord lipomas from inguinal hernias (44).

Sarcomas account for the majority of primary malignant lesions of the scrotum, with liposarcoma being one of the more common subtypes (45). MR imaging can prove useful in distinguishing liposarcoma from lipoma (46). Liposarcoma, even when well differentiated, frequently demonstrates thickened septa or enhancing soft-tissue components (Fig 12), some of which appear almost completely solid. Scrotal liposarcomas tend to be larger than scrotal lipomas and may demonstrate local invasion or evidence of metastatic disease as additional distinguishing characteristics.

A variety of lymphatic and vascular malformations may be seen in the scrotum. Lymphan-

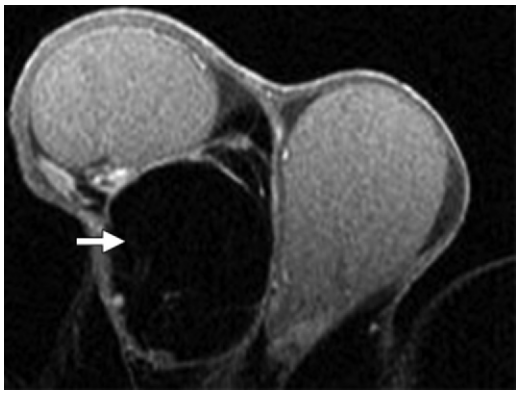

Figure 11. Lipoma of the spermatic cord in a 22-year-old man. Axial postcontrast fat-saturated T1-weighted MR image demonstrates complete fat saturation of a scrotal mass (arrow), in contrast to the higher-signal-intensity testicles.

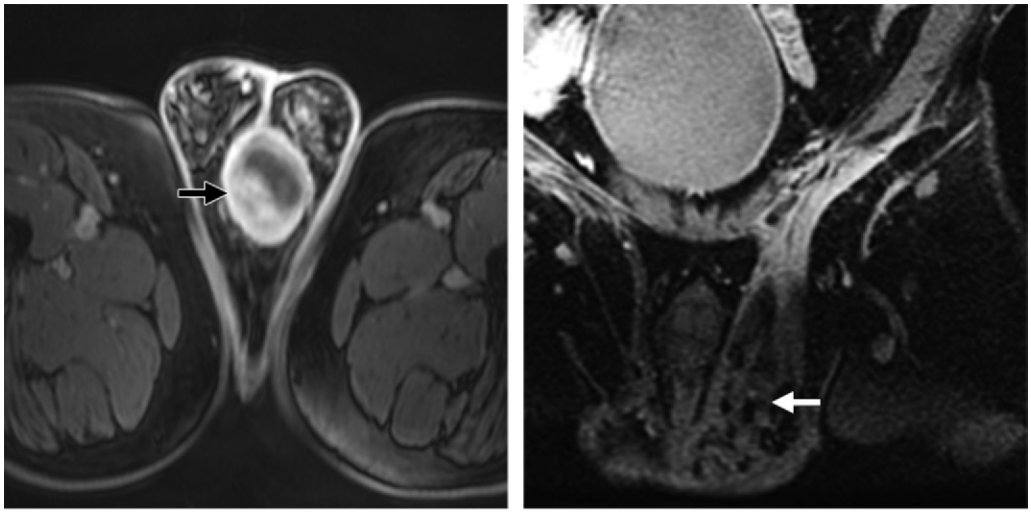

a. **b.**

Figure 12. Liposarcoma of the spermatic cord in a 63-year-old man. **(a)** Axial postcontrast T1-weighted MR image demonstrates an enhancing scrotal mass (arrow), which was surgically confirmed to be a dedifferentiated liposarcoma. **(b)** Coronal postcontrast fat-saturated T1-weighted MR image in a different patient demonstrates an irregular, enhancing soft-tissue mass with internal lipid in the left side of the scrotum (arrow), a finding that was also confirmed to be a scrotal liposarcoma.

gioma–lymphatic malformations consist of dilated lymphatic channels caused by occlusion of the normal drainage pathways, whether congenital or secondary to trauma, surgery, or infection. There is disagreement in the literature as to whether these masses represent true tumors that undergo endothelial hyperplasia or are simply malformations of lymphatic vascular pathways (47). At MR imaging, these masses appear as multiloculated cystic lesions, which can be quite large. They do not communicate with the peritoneal cavity and, like lymphatic malformations elsewhere in the body, demonstrate multiple thin septa with fluid-fluid levels (Fig 13). These masses appear predominantly T2 hyperintense and T1 hypointense due to their cystic nature. MR imaging can prove useful both in characterizing the mass, which may potentially be mistaken for a complex hydrocele at US, and in defining the extent of involvement prior to any anticipated intervention.

Hemangiomas are benign vascular malformations composed of dilated vascular channels with abnormal growth of the endothelial cells. Although hemangiomas are relatively common, they rarely involve the scrotum (<1% of cases) (48). The majority of hemangiomas manifest during childhood and, depending on the subtype, may enlarge as the child grows. If symptoms are present, surgery may be considered. In such cases, imaging is usually warranted to assess the full extent of involvement. At MR imaging, hemangiomas appear as lobulated soft-tissue masses that are hyperintense on T2-weighted images, hypointense on T1-weighted images, and typically demonstrate nodular areas of enhancement (Fig 14). Phleboliths (if present) appear as small, rounded areas of signal void. MR imaging can aid in the diagnosis and can show the extent of local involvement and help identify other vascular masses in patients with syndromes such as Klippel-Trénaunay syndrome.

Figure 13. Lymphangioma in a 19-year-old man. Axial T2-weighted MR image demonstrates a cystic scrotal mass with multiple septa and fluid-fluid levels (arrow).

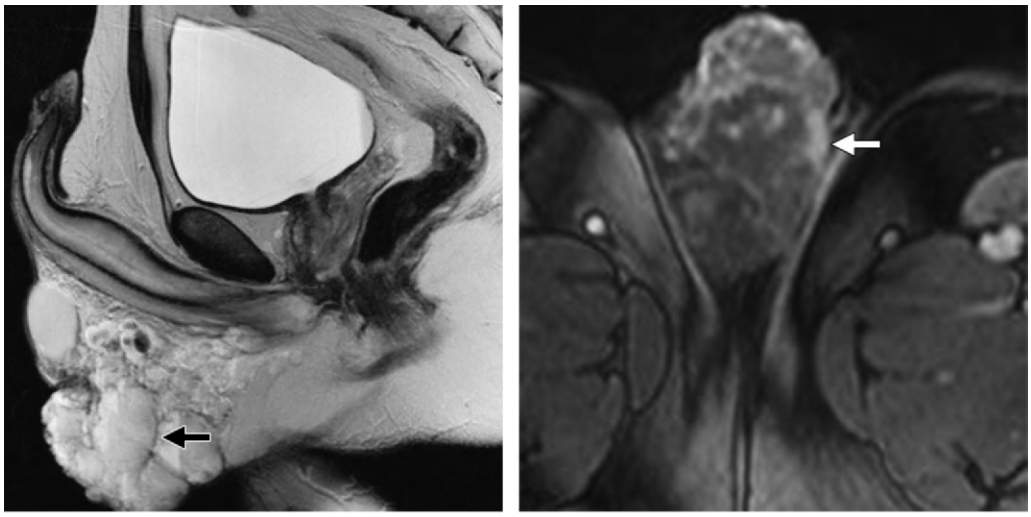

a. **b.**

Figure 14. Scrotal hemangioma in a 27-year-old man. Sagittal T2-weighted MR image **(a)** and axial post-contrast T1-weighted MR image **(b)** demonstrate a lobulated, T2-hyperintense mass with nodular areas of enhancement (arrow).

Scrotal arteriovenous malformations are rare vascular malformations consisting of enlarged tangles of abnormal arteries and draining veins without an intervening capillary bed. There are a small number of case reports in the literature describing scrotal arteriovenous malformations, most of which were found during workup for a scrotal mass or in patients with infertility, although a few patients presented with active bleeding (49). At MR imaging, the mass appears as a tangle of abnormal vessels, frequently with flow voids seen on both T1- and T2-weighted images. There is no associated soft-tissue mass. The surrounding soft tissue may demonstrate T2 hyperintensity due to edema (Fig 15). Following contrast material administration, there will be robust enhancement of the vascular mass similar to that of other vessels. The draining veins are typically larger than the feeding arteries. MR angiographic techniques, including time-resolved imaging, can be useful for identifying feeding arteries before surgery or angioembolization is performed.

Varicoceles, defined as abnormally dilated veins of the pampiniform plexus, are the most common palpable mass in the scrotal sac, occurring in up to 15% of all men. Most are left sided, and bilateral varicoceles are seen in approximately 15% of patients (50). Most varicoceles are idiopathic, related to incompetent valves. Rarely, especially if isolated on the right side, varicoceles can be secondary to obstruction of testicular veins by retroperitoneal masses. US is the imaging modality of choice in patients with suspected varicoceles. However, because of their prevalence, varicoceles are routinely encountered at scrotal MR imaging performed

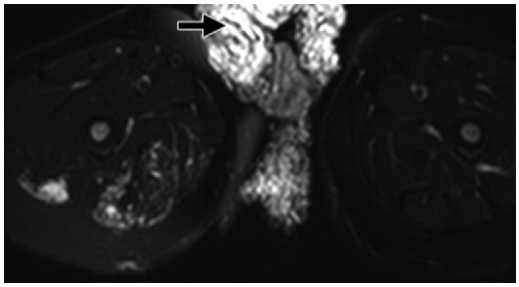

Figure 15. Scrotal arteriovenous malformation in a 41-year-old man. Axial fat-saturated T2-weighted MR image shows a large tangle of dilated tubular vessels involving the scrotum (arrow). MR imaging is performed prior to surgery or embolization to evaluate lesion extent.

Figure 16. Varicocele in a 44-year-old man. Sagittal T2-weighted MR image shows dilated paratesticular veins (white arrow) with extension into the testes (black arrow).

Figure 17. Adenomatoid tumor of the epididymis in a 24-year-old man. Coronal T2-weighted MR image show a well-defined paratesticular mass (arrow) with homogeneous signal intensity lower than that of the normal testes.

for other indications. At MR imaging, varicoceles manifest as dilated paratesticular veins, typically with T2 hyperintensity and without associated flow voids (Fig 16).

Adenomatoid tumors are the second most common benign neoplasms of the scrotum after lipoma (11). The majority of adenomatoid tumors arise in the epididymis, although these tumors have also been reported elsewhere in the scrotum. The cause of these lesions is unclear, but pathologic analysis shows that they are composed of irregular tubules lined with epithelial or endothelial cells. At MR imaging, these masses are typically well demarcated and hypointense relative to the testes on T2-weighted images (Fig 17). The masses enhance, but usually less than the adjacent testicle. MR imaging can be useful in confirming a paratesticular location, and the presence of enhancement can help confirm that the mass is a solid, soft-tissue neoplasm prior to surgical resection.

Numerous other neoplastic processes may rarely involve the scrotum. For instance, plexiform neurofibromas are benign tumors derived from all elements of the peripheral nerves. In the scrotum, they can sometimes be associated with proliferation of the overlying subcutaneous soft tissues, resulting in an "elephantiasis" appearance. Plexiform neurofibromas are seen only in patients with neurofibromatosis type 1 and appear at MR imaging as large, infiltrative masses that do not respect normal fascial spaces. The mass has a lobulated appearance with hyperintensity on T2-weighted images (Fig 18). On T1-weighted images, the mass is isointense relative to skeletal muscle and demonstrates enhancement following contrast material administration. There is no curative therapy, although resection is sometimes attempted for cosmetic or functional reasons. In such cases, MR imaging can prove useful in defining the extent of disease and aid in surgical planning. There is also a small risk of malignant degeneration, which can be suggested at MR imaging by rapid enlargement, especially in the setting of pain.

Testicular neoplasms are well evaluated with US, although a full description of US evaluation is beyond the scope of this article. However, these neoplasms are occasionally evaluated with MR imaging. Germ cell tumors are the most common testicular neoplasms, with seminomas being the most common subtype. At MR imaging, germ cell tumors appear as T2-hypointense

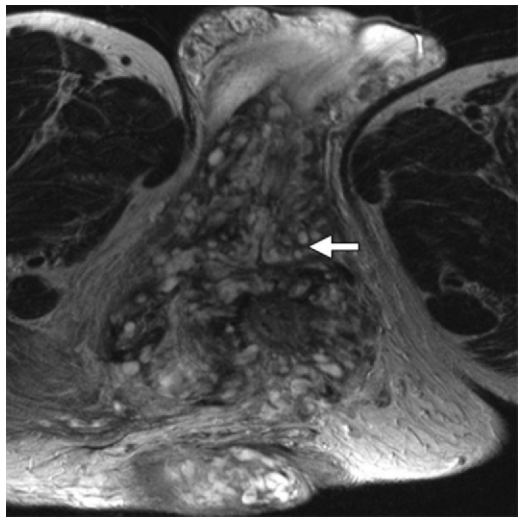

Figure 18. Scrotal plexiform neurofibroma in a 35-year-old man with neurofibromatosis type 1. Axial T2-weighted MR image shows a large plexiform neurofibroma (arrow) causing marked enlargement of the scrotum.

a. **b.**

Figure 19. Testicular germ cell tumor in a 23-year-old man. Axial T2-weighted **(a)** and coronal postcontrast T1-weighted **(b)** MR images demonstrate a large enhancing mass infiltrating the right testis (black arrow) and a necrotic tumor in the left testis (white arrow). Results of bilateral orchiectomy confirmed seminoma of both testes. Note the asymmetric enlargement of the right thigh **(a)** related to Klippel-Trénaunay-Weber syndrome. (Fig 19 courtesy of Andrés O'Brien, MD, Clínica Las Condes, Santiago, Chile.)

masses disturbing the normally T2-bright testicular parenchyma (Fig 19) and enhance following contrast material administration. A recent study suggests that dynamic contrast-enhanced MR imaging can be useful in distinguishing benign from malignant testicular neoplasms (51), with malignant neoplasms showing rapid and increased early enhancement with more rapid washout than the surrounding background. Although more work needs to be done in this area, accurate preoperative differentiation of benign from malignant neoplasms at MR imaging could have a profound impact on patient management, with malignant neoplasms leading to orchiectomy and benign lesions being either observed or enucleated.

Lymphoma is the most common secondary neoplasm involving the testes and the most common bilateral tumor. At MR imaging, lymphoma manifests as one or more T2-hypointense masses with enhancement following contrast material administration (Fig 20). At DW imaging, lymphoma appears hyperintense with corresponding decreased values on the ADC map, similar to its appearance elsewhere in the body (52).

Penis

Penile cancer primarily affects older men and is almost three times more common in uncircumcised males, making the presence of the foreskin the most important risk factor (51,52). Poor hygiene can increase the accumulation of smegma, also contributing to overall risk. Additional risk factors include phimosis, inflammatory conditions such as lichen sclerosus, and human papillomavirus 16

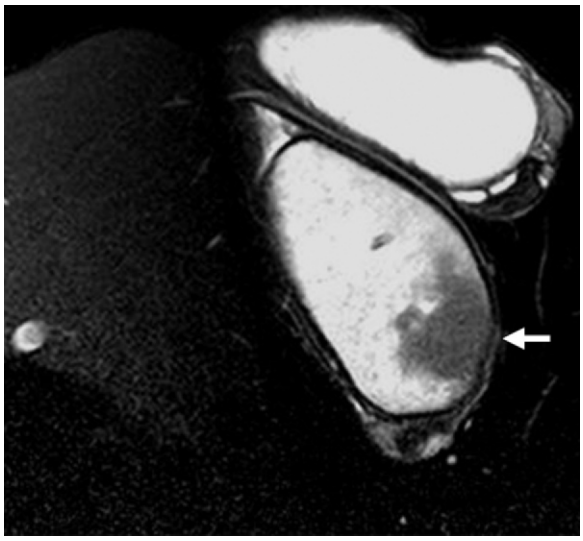

Figure 20. Testicular lymphoma in a 30-year-old man. Coronal fat-saturated T2-weighted MR image shows a round, hypointense mass in the testis (arrow), a finding that proved to be large cell non-Hodgkin lymphoma.

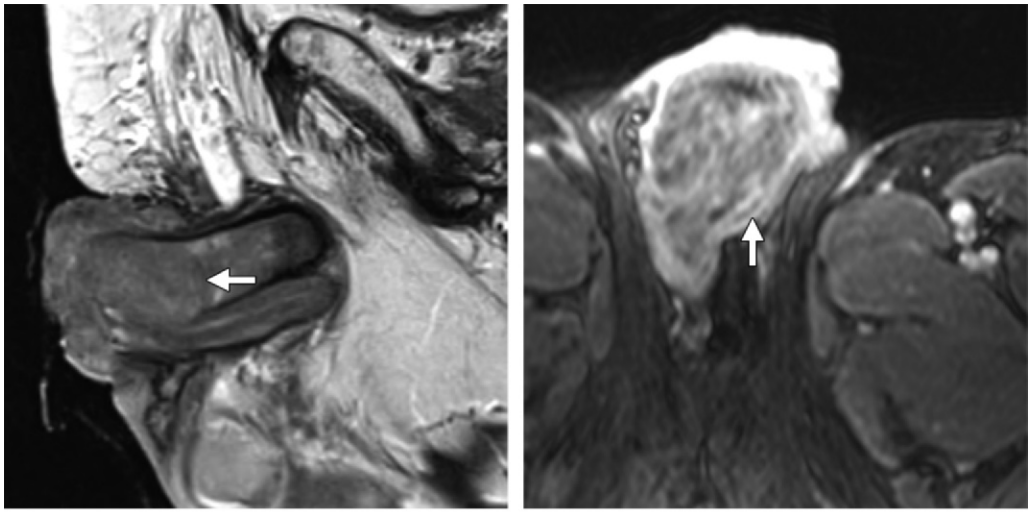

a. **b.**

Figure 21. Squamous cell carcinoma of the penis. **(a)** Sagittal T2-weighted MR image demonstrates a large, heterogeneously hypointense mass (arrow) involving the penile shaft, with invasion of the corpus cavernosum. **(b)** Axial postcontrast fat-saturated T1-weighted MR image in a different patient demonstrates a heterogeneously enhancing penile mass (arrow).

and 18 (51,52). The majority of penile cancers are squamous cell carcinomas, and most penile cancers arise in the glans or prepuce. Metastatic disease is usually to the local lymphatic system and, depending on tumor location, can affect both inguinal and pelvic chains. Lymph node involvement is the most important prognostic indicator and is frequently bilateral (51). Patients without nodal disease and with clear surgical margins at penectomy have excellent 5-year survival rates. However, survival rates decrease with progressive nodal involvement, to the point that studies have shown a 5-year survival rate of zero for patients with pelvic nodal disease (51,53). It should be noted, however, that concomitant infection is not unusual in patients with penile cancer, and differentiation between reactive lymphadenopathy and metastatic disease is not always possible on the basis of imaging findings alone, sometimes warranting fine-needle aspiration or biopsy.

At MR imaging, penile cancer usually appears as an infiltrative mass that is hypointense on T1- and T2-weighted images, with enhancement following contrast material administration (Fig 21). MR imaging is useful for defining the extent of penile cancer and assessing for invasion of the corpora cavernosa and/or urethra. Close attention should be paid to inguinal and pelvic lymph nodes, given the important prognostic implications of nodal involvement.

Urethral carcinomas can also occur in the penis, with most arising in the bulbous or membranous portions of the urethra (21,53). Occasionally, tumors will arise in the fossa navicularis. Most

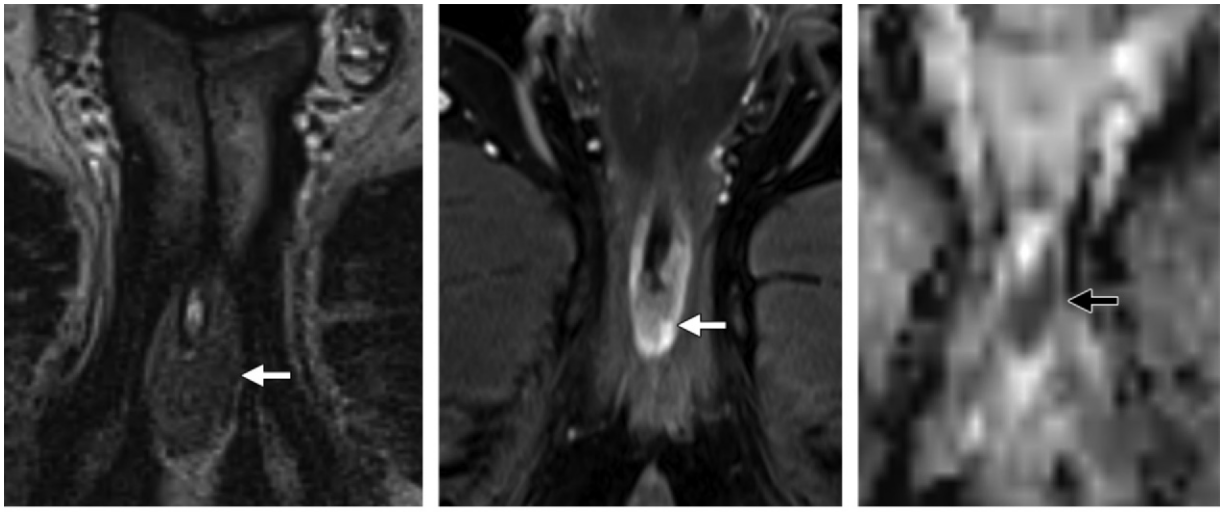

a. b. c.

Figure 22. Urethral squamous cell carcinoma in a 78-year-old man. Axial T2-weighted **(a)** and postcontrast T1-weighted **(b)** MR images and ADC map **(c)** demonstrate an enhancing mass (arrow) at the base of the penis in the expected location of the bulbomembranous junction of the urethra, with associated diffusion restriction.

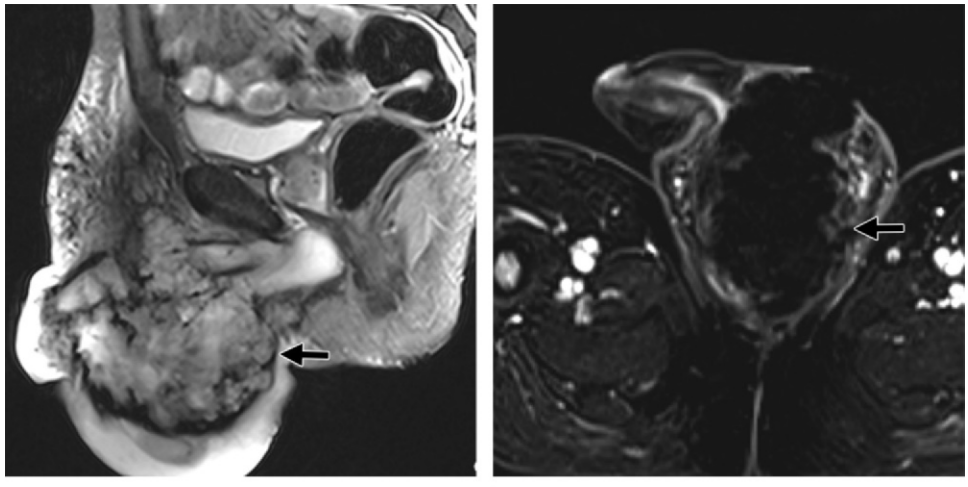

a. b.

Figure 23. Epithelioid sarcoma. Sagittal T2-weighted **(a)** and axial postcontrast T1-weighted **(b)** MR images demonstrate a large, heterogeneously enhancing mass (arrow) engulfing the scrotum and penis.

urethral carcinomas in the penis are squamous cell carcinomas, although transitional cell carcinoma and adenocarcinoma can also occur. Underlying strictures and chronic infectious or inflammatory processes are thought to be predisposing factors.

Penile urethral cancers appear hypointense relative to the corpora on T2-weighted images (Fig 22). There is typically contrast enhancement, and there may be diffusion restriction, with increased signal on DW images and corresponding low values on the ADC map (Fig 22c). These tumors can be differentiated from other penile tumors on the basis of their typical location in the bulbomembranous portion of the urethra and their being centered in the corpus spongiosum and/or urethra.

Sarcomas can also rarely arise in the penis. Subtypes include epithelioid sarcoma, leiomyosarcoma, rhabdomyosarcoma, and Kaposi sarcoma. Together, these tumors account for approximately 5% of all penile malignancies (21,54). The imaging appearance of sarcomas can vary. They are frequently large, locally invasive masses that tend to be isointense relative to skeletal muscle on T1-weighted images and hyperintense on T2-weighted images, with enhancement following contrast material administration (Fig 23).

Metastatic disease to the penis is rare. The most common primary tumors are those of the urogenital system, including prostate and bladder cancer (55,56). Like other penile tumors, metastases typically appear hypointense relative to the corpora on T2-weighted images, with varying degrees of enhancement. Diffusion restriction may also be present (Fig 24).

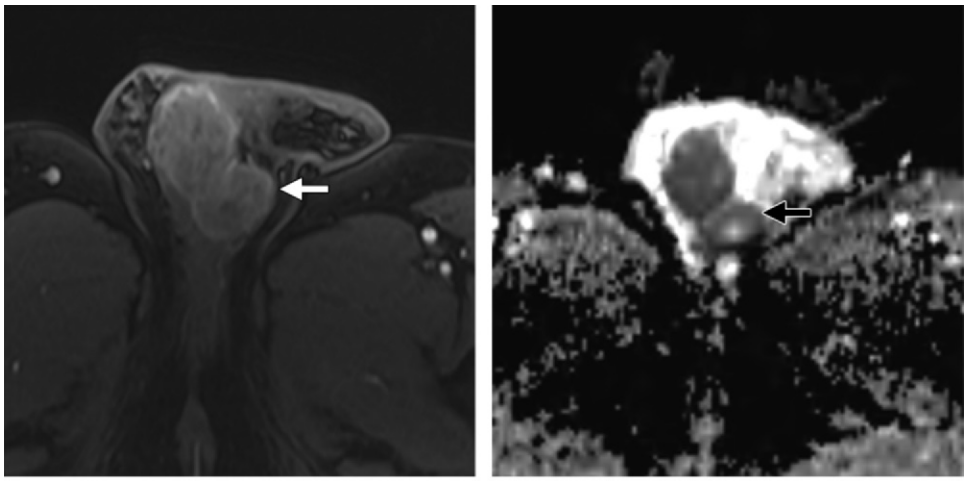

a. b.

Figure 24. Metastasis to the penis from a primary transitional cell carcinoma of the bladder in a 65-year-old man. Axial postcontrast T1-weighted MR image **(a)** and ADC map **(b)** demonstrate two enhancing masses at the base of the penis (arrow), with associated diffusion restriction.

Conclusion

US remains the primary modality for imaging of the penis and scrotum. However, US is limited in its ability to help characterize soft tissue, is user dependent, and sometimes has a limited useful FOV. MR imaging has emerged as the dominant problem-solving imaging modality in this setting and is increasingly being used by urologists. Advantages of MR imaging include the ability to help characterize soft tissue, thereby aiding in the differentiation of benign from malignant tumors or pseudotumors. For instance, the ability of MR imaging to clearly depict fat can aid in the diagnosis of lipoma or liposarcoma. Susceptibility artifacts related to gas or blood products can help identify infectious processes such as Fournier gangrene or hematomas. MR imaging has superior soft-tissue contrast relative to US and can clearly demonstrate small anatomic structures, such as the tunica albuginea, thereby aiding in the evaluation of patients with trauma and suspected penile fracture as well as patients with inflammatory conditions such as Peyronie disease. MR imaging is frequently used to help stage penile and scrotal tumors. Advanced techniques such as DW imaging are playing a more significant role and could potentially help characterize abscesses, identify sites of malignancy, and localize undescended testicles, although further research is necessary to validate these techniques.

References

1. Gottesman JE, Sample WF, Skinner DG, Ehrlich RM. Diagnostic ultrasound in the evaluation of scrotal masses. J Urol 1977;118(4):601–603.
2. Dogra VS, Gottlieb RH, Oka M, Rubens DJ. Sonography of the scrotum. Radiology 2003;227(1):18–36.
3. Krishnaswami S, Fonnesbeck C, Penson D, McPheeters ML. Magnetic resonance imaging for locating nonpalpable undescended testicles: a meta-analysis. Pediatrics 2013;131(6):e1908–e1916.
4. Muglia V, Tucci S Jr, Elias J Jr, Trad CS, Bilbey J, Cooperberg PL. Magnetic resonance imaging of scrotal diseases: when it makes the difference. Urology 2002;59(3):419–423.
5. Serra AD, Hricak H, Coakley FV, et al. Inconclusive clinical and ultrasound evaluation of the scrotum: impact of magnetic resonance imaging on patient management and cost. Urology 1998;51(6):1018–1021.
6. Lont AP, Besnard AP, Gallee MP, van Tinteren H, Horenblas S. A comparison of physical examination and imaging in determining the extent of primary penile carcinoma. BJU Int 2003;91(6):493–495.
7. Healy JC. Penis. In: Standing S, ed. Gray's anatomy. London, England: Elsevier, 2005; 1315–1317.
8. Kaneko K, De Mouy EH, Lee BE. Sequential contrast-enhanced MR imaging of the penis. Radiology 1994;191(1):75–77.
9. Healy JC. Spermatic cords and scrotum. In: Standing S, ed. Gray's anatomy. London, England: Elsevier, 2005; 1313–1314.
10. Avery LL, Scheinfeld MH. Imaging of penile and scrotal emergencies. RadioGraphics 2013;33(3):721–740.
11. Cassidy FH, Ishioka KM, McMahon CJ, et al. MR imaging of scrotal tumors and pseudotumors. RadioGraphics 2010;30(3):665–683.
12. Scardino E, Villa G, Bonomo G, et al. Magnetic resonance imaging combined with artificial erection for local staging of penile cancer. Urology 2004;63(6):1158–1162.
13. Kirkham AP, Illing RO, Minhas S, Minhas S, Allen C. MR imaging of nonmalignant penile lesions. RadioGraphics 2008;28(3):837–853.
14. Linet OI, Ogrinc FG. Efficacy and safety of intracavernosal alprostadil in men with erectile dysfunction. The Alprostadil Study Group. N Engl J Med 1996;334(14):873–877.
15. Sawyer-Glover AM, Shellock FG. Pre-MRI procedure screening: recommendations and safety considerations for biomedical implants and devices. J Magn Reson Imaging 2000;12(1):92–106.
16. Shellock FG, Kanal E. Magnetic resonance: bioeffects, safety and patient management. Philadelphia, Pa: Lippincott Williams & Wilkins, 1996; 144–205.
17. Narra VR, Howell RW, Goddu SM, Rao DV. Effects of a 1.5-Tesla static magnetic field on spermatogenesis and embryogenesis in mice. Invest Radiol 1996;31(9):586–590.
18. Shellock FG, Rothman B, Sarti D. Heating of the scrotum by high-field-strength MR imaging. AJR Am J Roentgenol 1990;154(6):1229–1232.
19. Sawh SL, O'Leary MP, Ferreira MD, Berry AM, Maharaj D. Fractured penis: a review. Int J Impot Res 2008;20(4):366–369.

20. Boudghene F, Chhem R, Wallays C, Bigot JM. MR imaging in acute fracture of the penis. Urol Radiol 1992;14(3):202–204.
21. Pretorius ES, Siegelman ES, Ramchandani P, Banner MP. MR imaging of the penis. RadioGraphics 2001;21(Spec No):S283–S298; discussion S298–S299.
22. Hoag NA, Hennessey K, So A. Penile fracture with bilateral corporeal rupture and complete urethral disruption: case report and literature review. Can Urol Assoc J 2011;5(2):E23–E26.
23. Agarwal MM, Singh SK, Sharma DK, et al. Fracture of the penis: a radiological or clinical diagnosis? a case series and literature review. Can J Urol 2009;16(2):4568–4575.
24. Yapanoglu T, Aksoy Y, Adanur S, Kabadayi B, Ozturk G, Ozbey I. Seventeen years' experience of penile fracture: conservative vs. surgical treatment. J Sex Med 2009;6(7):2058–2063.
25. Jack GS, Garraway I, Reznichek R, Rajfer J. Current treatment options for penile fractures. Rev Urol 2004;6(3):114–120.
26. Bradley WG. MR appearance of hemorrhage in the brain. Radiology 1993;189(1):15–26.
27. Barthold JS. Abnormalities of the testes and scrotum and their surgical management. In: Wein AJ, ed. Campbell-Walsh urology. 10th ed. Philadelphia, Pa: Saunders Elsevier, 2011.
28. Montgomery JS, Bloom DA. The diagnosis and management of scrotal masses. Med Clin North Am 2011;95(1):235–244.
29. Guichard G, El Ammari J, Del Coro C, et al. Accuracy of ultrasonography in diagnosis of testicular rupture after blunt scrotal trauma. Urology 2008;71(1):52–56.
30. Kim SH, Park S, Choi SH, Jeong WK, Choi JH. The efficacy of magnetic resonance imaging for the diagnosis of testicular rupture: a prospective preliminary study. J Trauma 2009;66(1):239–242.
31. Kogan SJ. Cryptorchidism. In: Kelalis PP, King LR, Gelman AB, eds. Clinical pediatric urology. 2nd ed. Philadelphia, Pa: Saunders, 1985; 864–887.
32. Kantarci M, Doganay S, Yalcin A, Aksoy Y, Yilmaz-Cankaya B, Salman B. Diagnostic performance of diffusion-weighted MRI in the detection of nonpalpable undescended testes: comparison with conventional MRI and surgical findings. AJR Am J Roentgenol 2010;195(4):W268–W273.
33. Nguyen HT. Bacterial infections of the genitourinary tract. In: Tanagho EA, McAninch JW, eds. Smith's general urology. New York, NY: McGraw-Hill, 2004; 203–227.
34. Hartmann M, Jansen O, Heiland S, Sommer C, Münkel K, Sartor K. Restricted diffusion within ring enhancement is not pathognomonic for brain abscess. AJNR Am J Neuroradiol 2001;22(9):1738–1742.
35. Chan JH, Tsui EY, Luk SH, et al. Diffusion-weighted MR imaging of the liver: distinguishing hepatic abscess from cystic or necrotic tumor. Abdom Imaging 2001;26(2):161–165.
36. O'Malley RB, Al-Hawary MM, Kaza RK, Wasnik AP, Liu PS, Hussain HK. Rectal imaging. II. Perianal fistula evaluation on pelvic MRI: what the radiologist needs to know. AJR Am J Roentgenol 2012;199(1):W43–W53.
37. Morpurgo E, Galandiuk S. Fournier's gangrene. Surg Clin North Am 2002;82(6):1213–1224.
38. Levenson RB, Singh AK, Novelline RA. Fournier gangrene: role of imaging. RadioGraphics 2008;28(2):519–528.
39. Jalkut M, Gonzalez-Cadavid N, Rajfer J. Peyronie's disease: a review. Rev Urol 2003;5(3):142–148.
40. Schwarzer U, Sommer F, Klotz T, Braun M, Reifenrath B, Engelmann U. The prevalence of Peyronie's disease: results of a large survey. BJU Int 2001;88(7):727–730.
41. Hauck EW, Hackstein N, Vosshenrich R, et al. Diagnostic value of magnetic resonance imaging in Peyronie's disease: a comparison both with palpation and ultrasound in the evaluation of plaque formation. Eur Urol 2003;43(3):293–299; discussion 299–300.
42. Helweg G, Judmaier W, Buchberger W, et al. Peyronie's disease: MR findings in 28 patients. AJR Am J Roentgenol 1992;158(6):1261–1264.
43. Kadioglu A, Akman T, Sanli O, Gurkan L, Cakan M, Celtik M. Surgical treatment of Peyronie's disease: a critical analysis. Eur Urol 2006;50(2):235–248.
44. Burkhardt JH, Arshanskiy Y, Munson JL, Scholz FJ. Diagnosis of inguinal region hernias with axial CT: the lateral crescent sign and other key findings. RadioGraphics 2011;31(2):E1–E12.
45. Beccia DJ, Krane RJ, Olsson CA. Clinical management of non-testicular intrascrotal tumors. J Urol 1976;116(4):476–479.
46. Gaskin CM, Helms CA. Lipomas, lipoma variants, and well-differentiated liposarcomas (atypical lipomas): results of MRI evaluations of 126 consecutive fatty masses. AJR Am J Roentgenol 2004;182(3):733–739.
47. Huang HY, Ho CC, Huang PH, Hsu SM. Co-expression of VEGF-C and its receptors, VEGFR-2 and VEGFR-3, in endothelial cells of lymphangioma: implication in autocrine or paracrine regulation of lymphangioma. Lab Invest 2001;81(12):1729–1734.
48. Lin CY, Sun GH, Yu DS, Wu CJ, Chen HI, Chang SY. Intrascrotal hemangioma. Arch Androl 2002;48(4):259–265.
49. Zachariah JR, Gupta AK, Lamba S. Arteriovenous malformation of the scrotum: is preoperative angioembolization a necessity? Indian J Urol 2012;28(3):329–334.
50. Cornud F, Belin X, Amar E, Delafontaine D, Hélénon O, Moreau JF. Varicocele: strategies in diagnosis and treatment. Eur Radiol 1999;9(3):536–545.
51. Singh AK, Saokar A, Hahn PF, Harisinghani MG. Imaging of penile neoplasms. RadioGraphics 2005;25(6):1629–1638.
52. Pow-Sang MR, Benavente V, Pow-Sang JE, et al. Cancer of the penis. Cancer Contr 2002;9(4):305–314.
53. Ravi R. Correlation between the extent of nodal involvement and survival following groin dissection for carcinoma of the penis. Br J Urol 1993;72(5 pt 2):817–819.
54. Lucia MS, Miller GJ. Histopathology of malignant lesions of the penis. Urol Clin North Am 1992;19(2):227–246.
55. Griffin JH, Wheeler JS Jr, Olson M, Melian E. Prostate carcinoma metastatic to the penis: magnetic resonance imaging and brachytherapy. J Urol 1996;155(5):1701–1702.
56. Demuren OA, Koriech O. Isolated penile metastasis from bladder carcinoma. Eur Radiol 1999;9(8):1596–1598.